

Residual life estimation of fabricated humidity sensors using different artificial intelligence techniques

C. BHARGAVA¹, J. AGGARWAL², and P.K. SHARMA^{3*}

¹Department of ECE, Lovely Professional University, Phagwara, Punjab 144411, India

²CSS Corp., Chennai, Tamilnadu, 600058, India

³Department of PS, Lovely Professional University, Phagwara, Punjab 144411, India

Abstract. Background: a humidity sensor is used to sense and measure the relative humidity of air. A new composite system has been fabricated using environmental pollutants such as carbon black and low-cost zinc oxide, and it acts as a humidity sensor. Residual life of the sensor is calculated and an expert system is modelled. For properties and nature confirmation, characterization is performed, and a sensing material is fabricated. Methodology: characterization is performed on the fabricated material. Complex impedance spectroscopy (CIS), Fourier transform infrared spectroscopy (FTIR), X-ray diffraction (XRD) and scanning electron microscopy (SEM) are all used to confirm the surface roughness, its composite nature as well as the morphology of the composite. The residual lifetime of the fabricated humidity sensor is calculated by means of accelerated life testing. An intelligent model is designed using artificial intelligence techniques, including the artificial neural network (ANN), fuzzy inference system (FIS) and adaptive neuro-fuzzy inference system (ANFIS). Results: maximum conductivity obtained is 6.4×10^{-3} S/cm when zinc oxide is doped with 80% of carbon black. Conclusion: the solid composite obtained possesses good humidity-sensing capability in the range of 30–95%. ANFIS exhibits the maximum prediction accuracy, with an error rate of just 1.1%.

Key words: composite material, artificial intelligence, humidity sensor, accelerated life testing, SEM.

1. Introduction

The first silicon-based integrated circuit was introduced in 1964 by Harwick Johnson. Since then, IC technology has been advancing at a very rapid rate. Nowadays, emerging branches, e.g. solid-state electronics, become responsible for the invention of devices such as the transistor. Nanotechnology has brought about a variety of new composite materials characterized by better conductivity and properties such as improved stability in relation to temperature, high melting and boiling points, less activation energy etc., as compared to the conventional material used. Solid state electrolytes are observed to have high electrical conductivity, which makes them an excellent material for designing electrical and electronic products such as relays, switches etc. Doping or adding impurities is considered one of the methods to enhance conductivity or other features of the material [1]. A variety of studies have been conducted as part of material science to extract new materials through doping inadequate amounts in order to get the best composition [2].

Carbon black is one of the most prominent environmental pollutants and an easily available insulating material produced due to combustion of solid material. It exhibits amorphous properties, and due to this, doping with carbon affects conductivity of the composite material in a visible manner [3]. Zinc oxide (ZnO) is one of promising materials to be used in elec-

trochemical capacitors electrodes. This oxide material has been widely applied in optoelectronic and electronic devices, such as light-emitting devices, gas sensors and solar cells, so composite materials based on carbon and zinc oxide could become efficient electrode materials [4–7] for electrochemical capacitors.

Several techniques have been designated in previous studies for the production of zinc oxide. These include, for example: hydrothermal technique, laser ablation, sol-gel, chemical vapor deposition, thermal decomposition, combustion and electrochemical depositions [4–7]. The electrodeposition method is known as the efficient technique for the synthesis of nanostructures of ZnO due to its easiness, low-temperature procedure, high deposition amount, cheap method and appropriateness for large area substrate [6]. This method uses a very low potential or current to produce ZnO on any conductive substrate. In this deposition procedure, the thin layer measurements, structures and electrochemical characteristics could be adapted by a variety of operating parameters: current intensity, voltage applied, time of deposition and the electrodeposition bath [8]. Generally, in this deposition process, zinc chloride solutions or zinc nitrate solutions are used as a precursor [4–7]. In medical applications, it is utilized in skin ointments which are used to cure skin allergies. The sol-gel method, also used to form ZnO, is carried out using zinc acetate dehydrate and sodium hydroxide. Ethanol is used as a solvent for the process, along with distilled water to act as a medium [3]. Overall, the zinc content is 55.38% while the oxygen content remains at 44.62%. More recently, materials scientists and engineers have suggested and devised various methods of using this waste product for the synthesis of some useful composites.

*e-mail: pardeep.kumar1@lpu.co.in

Manuscript submitted 2018-01-05, revised 2018-02-27, initially accepted for publication 2018-04-03, published in February 2019.

In this paper, a sensor has been fabricated using both zinc oxide and carbon, and it exhibits good humidity- sensing capability. Three soft computing techniques have been considered for intelligent modelling. The experimental technique, i.e. accelerated life testing method, is used to compute the residual lifetime. A variety of artificial intelligence techniques, such as ANN, FIS and ANFIS, have been incorporated through MATLAB Simulink, which constitutes an intelligent model that predicts residual life of the fabricated sensor. The accuracy of these methods is computed with reference to the experimental technique.

2. Fabricating the humidity sensor

2.1. Sample preparation. For the preparation of a sample, zinc oxide has been prepared by means of the Sol-Gel method at the laboratory at a temperature of 343 K using NaOH and $Zn(NO_3)_2 \cdot 6H_2O$ in its purest form along with deionized water. For carbon black, fumes have been collected in a closed chamber to accumulate on the top lid through combustion. For the composite electrolyte, ten samples have been prepared [9]. Firstly, carbon black and zinc oxide were kept in a hot-air oven at a temperature of 423 K for activation purpose. This process takes nearly two hours, and after that both zinc oxide and carbon were mixed and grinded continuously for two hours, using a mortar and a pestle [10]. Palletization is performed with the use of a hydraulic palletizer with a pressure of 2.5 to 3.5 torr with the die having the cross-sectional area of 0.2 cm^2 for pallets and the thickness considered standing at approximately 3.5 mm. An optical photograph of the sensor is presented in Fig. 1.

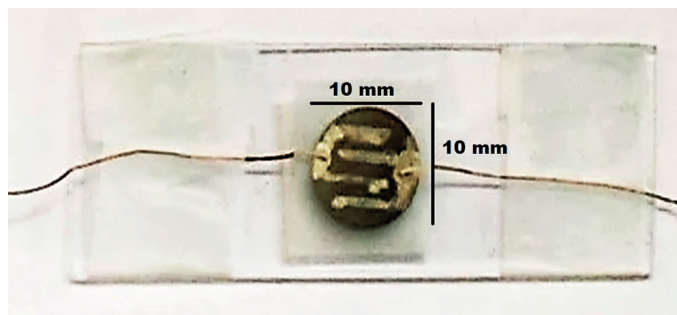


Fig. 1. Optical photograph of fabricated sensor

A variety of characterization tests confirm that the fabricated sensor acts as a humidity sensor.

3. Characterization techniques

To confirm the composite nature, surface morphology and conducting nature, a variety of tests are conducted on the fabricated sensor.

3.1. Complex impedance spectroscopy. The conducting behavior of a carbon black and zinc oxide composite is examined

using complex impedance spectroscopy [3]. Origin 7.1 software is used to convert the obtained data into graphical images. Further bulk resistance (R_b), has been calculated from the graph by determining the point where the semicircle corresponding to impedance intersects the x-axis.

In our laboratory, we used pressure-contacted stainless-steel electrodes and connected them to a CH instruments electrochemical workstation (model CHI604D) with a frequency range of 0.00001 Hz to 100 kHz. On the basis of this resistance value, maximum conductivity was determined amongst the ten samples. The values are listed in Table 1 below.

Table 1
Variation of conductivity at different carbon ratios

No.	ZnO-carbon ratio (w/w = 2gm)	Conductivity value (S/cm)
1.	20–80	0.0064
2.	30–70	0.000125
3.	40–60	0.000241
4.	50–50	0.000111
5.	60–40	0.00025
6.	70–30	0.000388
7.	80–20	0.0007
8.	90–10	0.000128
9.	Pure carbon	0.000109
10.	Pure ZnO	0.000005833

Out of the ten samples, maximum conductivity is observed for the 20–80 ratio, i.e. 20% of zinc and 80% of carbon black, giving conductivity of $6.4 \times 10^{-3} \text{ S/cm}$. It can be deduced from the table that with different ratios, different conductivity values are observed, and they show a non-linear relationship. The Cole-Cole plot for the 20–80 ratio has been shown in Fig. 2 below.

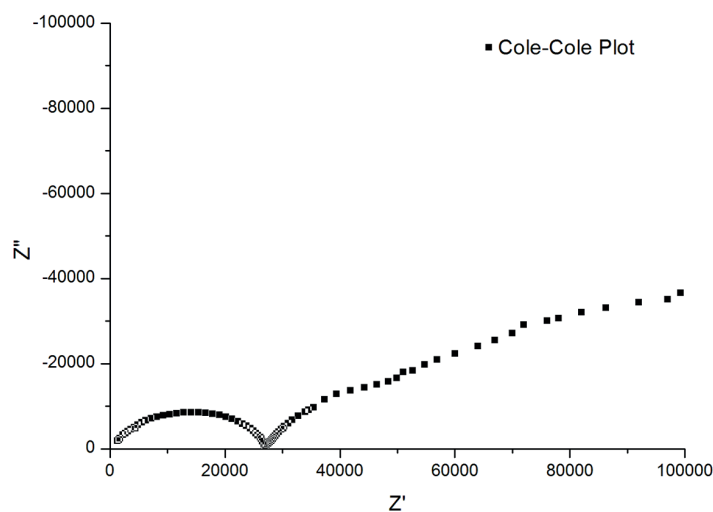


Fig. 2. Cole-Cole plot for maximum conducting composite

3.2. Fourier transform infrared spectroscopy. From observation of IR graphs, it can be deduced that:

- all the spikes and peaks from ZnO and carbon are also present in the ZnO-carbon composite;
- the curve for the composite covers all the slopes of the waveform;
- all the peaks of the composite can be attributed either to ZnO or to carbon.

The ZnO waveform shows two extra peaks. This is because the presence of even the tiniest of impurities in it as a sample can result in contamination already while performing the test.

Apart from the peaks of the parent materials, i.e. ZnO and carbon, the composite doesn't have any other peaks which would confirm that it is purely a composite of ZnO and carbon and that it exhibits the properties of both these materials [11]. Fig. 3 shows the FTIR result for ZnO, carbon and their composite.

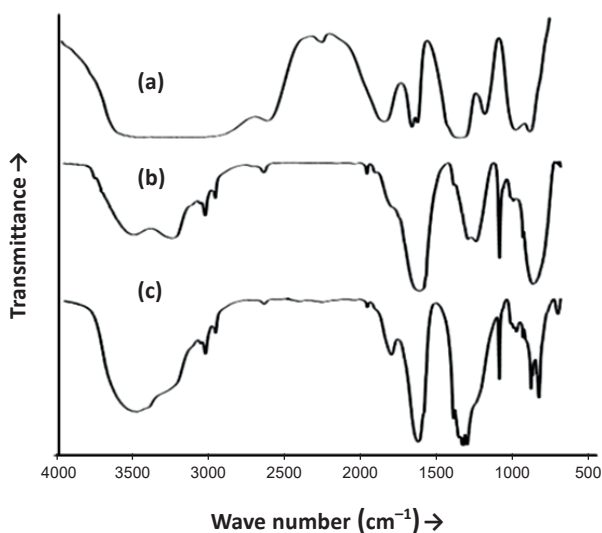


Fig. 3. FTIR characteristics graph for: (a) pure ZnO, (b) pure carbon, and (c) carbon-ZnO composite

3.3. X-ray diffraction. The X-ray diffraction test is performed to confirm the crystalline nature of the ZnO-carbon composite material. From the XRD graph, it is revealed that carbon is showing no extra spikes in its resultant graph, which confirms its amorphous nature [11]. Meanwhile, the zinc oxide spikes are very sharp as compared to carbon and all the peaks which are available in carbon as well as ZnO are present in the graph of the zinc oxide and carbon composite. This confirms that there are no impurities present in the composite and its composition is purely carbon and zinc oxide [12]. Also, it confirms the homogenous nature of the composite. The XRD waveform is presented in Fig. 4. The entirety of the zinc oxide and carbon composite diffraction peaks in Fig. 4b matched the ZnO ones very well (JCPDS/ICDD 36-1451).

3.4. Scanning electron microscopy (SEM). This test is conducted mainly to acquire surface images of the material. Hence

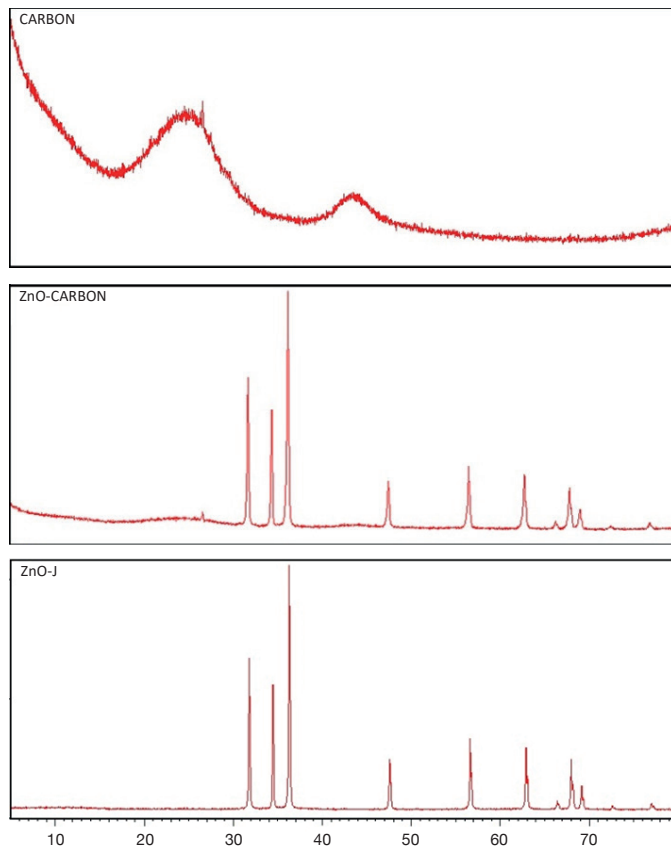


Fig. 4. XRD pattern of (a) pure carbon (b) ZnO-carbon (c) pure ZnO

in order to determine surface morphology, orientation as well as the surface roughness of the composite and parent material, SEM is performed [13]. Also, it confirms the presence of both the materials at micro-level in the composite [14]. For a SEM micrograph of carbon, the minimum size of the particle is 1 μm and the maximum size is 25 μm . SEM micrographs for ZnO, carbon and their composite are all shown in Fig. 5-7.

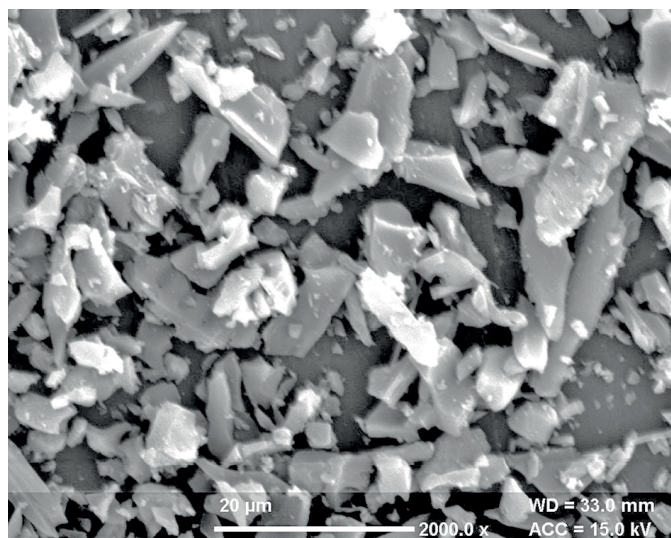


Fig. 5. SEM micrograph of carbon

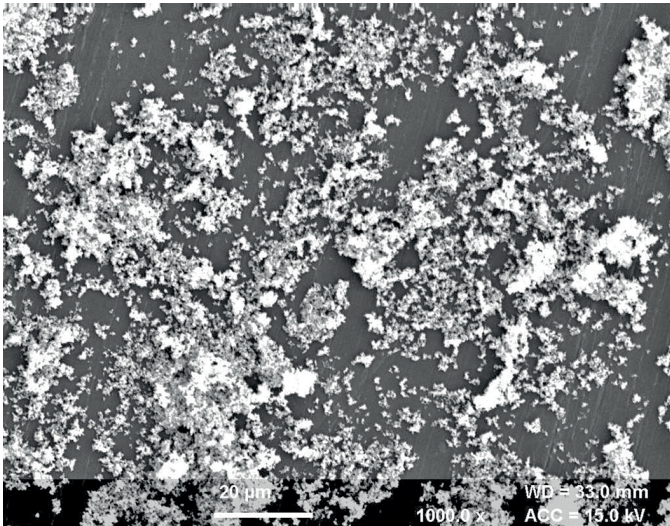


Fig. 6. SEM micrograph of zinc oxide

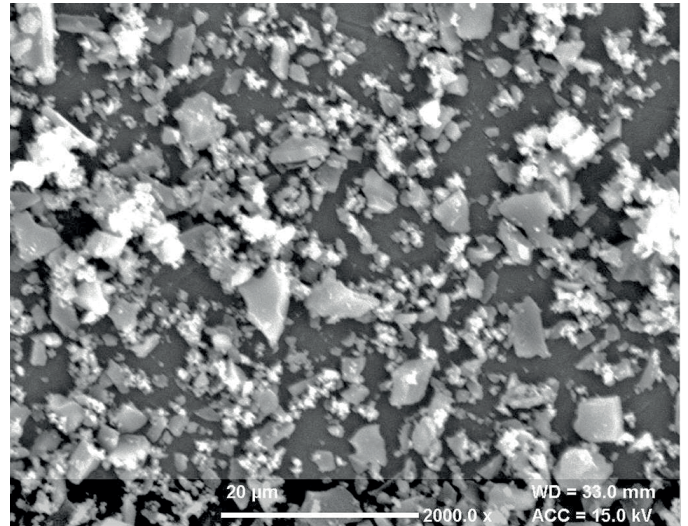


Fig. 7. SEM micrograph of ZnO-carbon composite

4. Humidity measurement

The overall range for this humidity sensor is between 30% RH and 95%RH, after which it will stop sensing.

This range is extracted and interpreted in terms of voltage, which is beneficial for further studies, in order to calculate its life [14]. Fig. 8 shows the result obtained from the experiment in the form of a graph.

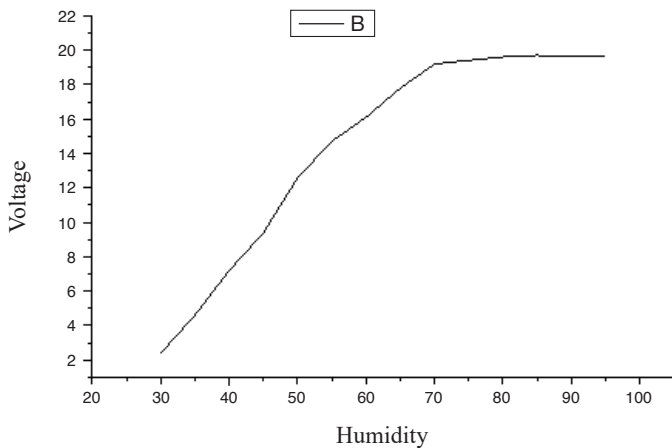


Fig. 8. Humidity versus voltage graph

Overall sensitivity of the sensor is 99.7%, which appears to stand for better efficiency.

5. Residual life estimation of fabricated sensor

Residual life estimation is an important aspect when successful operation is considered [15]. Determining the remaining useful life (RUL) helps estimate how long the sensor will work over time in order to avoid sudden failure of the sensor, as it may

lead to loss of necessary information. The Arrhenius method has been used to see the effect of temperature on the sensor and hence mean time between failures (MTBF) has been calculated [16].

Also, intelligent modelling has been used to design a smart system which can forecast the life using artificial intelligence techniques such as ANN, FIS and ANFIS [17].

5.1. Experimental technique. The accelerated life testing technique is used for calculating the sensor's residual lifetime [18]. A digital hot plate, sand and sensor samples are taken. Figure 9 illustrates the experimental setup for accelerated life testing, where 35 samples have been taken and covered in sand, so that uniform heating can be applied to all of them. All the samples have been kept under observation for 200 hr to check the effect



Fig. 9. Experimental setup for calculating residual lifetime

of temperature [19]. It is observed that after a certain time some of the samples are unable to withstand high temperature for a longer period [20].

The FIT (per 10^9 hours) has been calculated using an Arrhenius equation of the acceleration factor.

$$FIT(\lambda) = F/D.T.A_F \tag{1}$$

where:

F is the number of failures,

D is the number of sensors tested and T = test hours

A_F = acceleration factor = $\exp [E_a/k(1/T_{use}-1/T_{test})]$

E_a = activation energy (ev)

K = Boltzmann constant

T_{use} = use temperature, T_{test} = test temperature.

After calculating the failure rate [21], the MTBF corresponding to FIT was calculated as follows:

$$MTBF(h) = (1/\lambda) * 10^9 h. \tag{2}$$

The life calculated using the accelerated life testing method is summarized in Table 2.

Table 2
MTBF calculation using experimental technique

No.	Humidity (%RH)	Voltage (V)	Temperature (K)	Experimental method
1.	30	2.4	273	225.3
2.	35	4.6	278	132.1
3.	40	7.2	283	79.01
4.	45	9.4	288	48.07
5.	50	12.6	293	29.74
6.	55	14.7	298	18.7
7.	60	16.1	303	11.94
8.	65	17.8	308	7.74
9.	70	19.2	313	5.08
10.	75	19.4	318	3.38
11.	80	19.6	323	2.28
12.	85	19.7	328	1.55
13.	90	19.6	333	1.07
14.	95	19.7	338	0.75

6. Intelligent prediction of residual life using AI techniques

The artificial intelligence techniques are used to model an expert system that predicts the residual life of the humidity sensor [22]. The various techniques used for the expert system include artificial neural networks (ANN), fuzzy inference system (FIS) and adaptive neuro-fuzzy inference system (ANFIS) [23].

6.1. Artificial neural networks-based intelligent system. Artificial neural networks (ANN) can be considered non-linear operators that transform a set of suitably interpreted variables at their input into another set of numerical data at their output[24]. ANN use a mapping technique through which the network output is continuously updated, based on the minimum value of mean square error (MSE). This process is known as training [25].

The topology of the network used here is 3-10-1, i.e. 3 inputs, 1 output and 10 neurons in the hidden layer. These three inputs indicate humidity, voltage and temperature while the output marks life estimation [26]. The artificial neural network thus created is shown below in Fig. 10. Here, a total of fourteen samples are used for training and 10 have been used for testing [27]. The number of epochs taken are 1000 and best validation performance of 0.35 is observed at iteration 6.

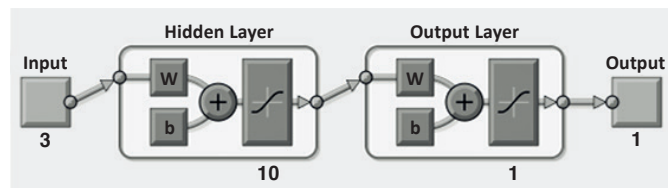


Fig. 10. ANN formed 3–10–1

6.2. Fuzzy logic-based intelligent system. The fuzzy inference system has an advantage over ANN in that it deals with linguistic variables and it is comparatively user-understandable [28]. Implementation of fuzzy is done using MATLAB Simulink [29]. The resultant membership function acquired is presented in Fig. 11. The corresponding membership function is defined for each input. Here, five membership functions (very

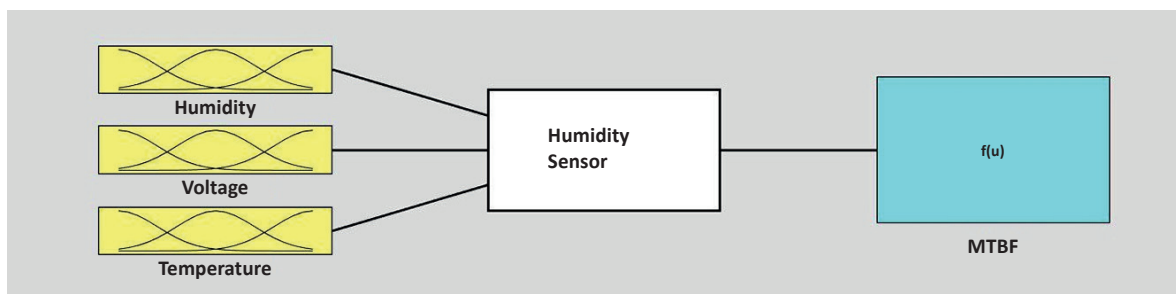


Fig. 11. Fuzzy model for intelligent system

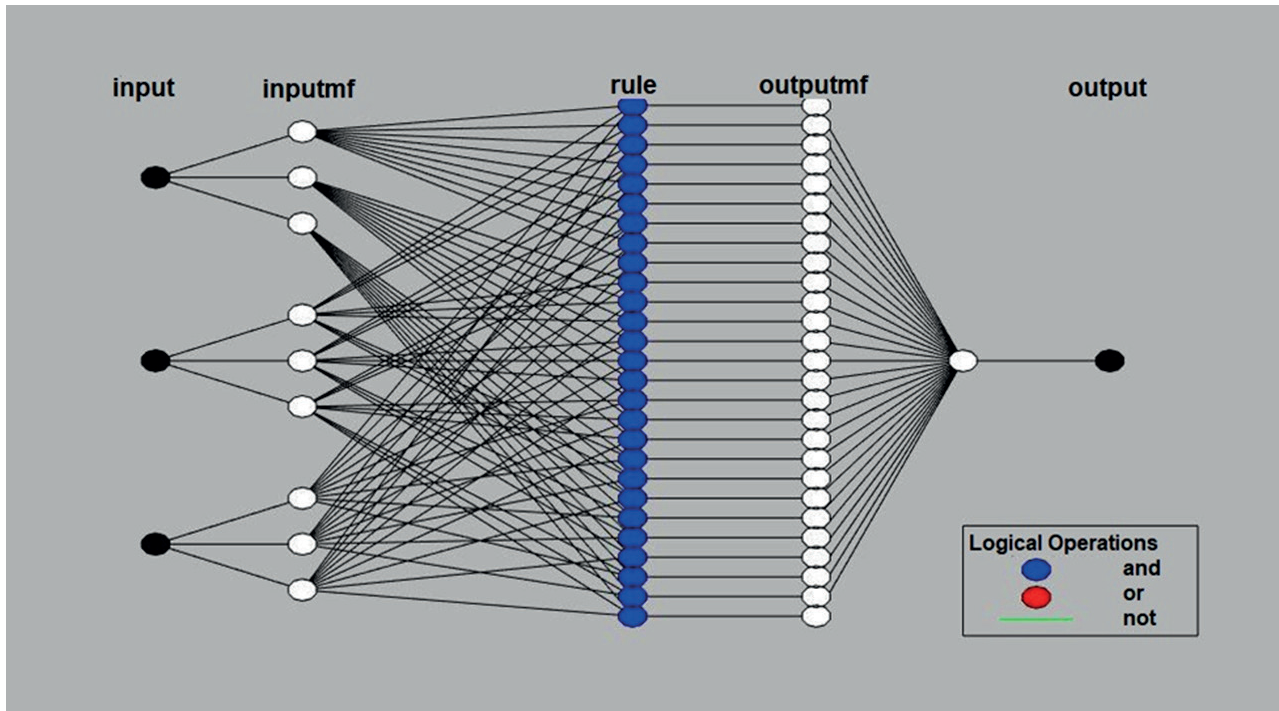


Fig. 12. ANFIS intelligent system

low, low, medium, high and very high) are used [30]. Based on these membership functions, 25 rules have been designed using the FIS rules generator [31].

6.3. ANFIS-based intelligent system. ANFIS is also one of the techniques used prominently for intelligent modelling [32]. The advantage of ANFIS lies in that it combines the properties of both the fuzzy inference system and artificial neural networks [33]. The residual lifetime data are uploaded into MATLAB Simulink, and then the system is trained and tested [34].

Another advantage of ANFIS is that there emerges no need to formulate the fuzzy rules as the adaptive system constructs the rules itself, through the learning [35]. With the help of the rule viewer, residual lifetime can be predicted [36]. The ANFIS network formed is presented in Fig. 12.

7. Results and discussion

A new composite material has been fabricated using carbon black and zinc oxide. The characterization tests confirm its composite nature and sensing behavior. The life of the fabricated sensor is analyzed using accelerated life testing. An expert system is modelled using artificial intelligence techniques, and it predicts the residual life of the sensor. The accuracy of this system is measured by keeping the experimental value as the reference one, which proves ANFIS as the most accurate artificial intelligence technique. Comparative analysis of all the techniques is presented in Fig. 13.

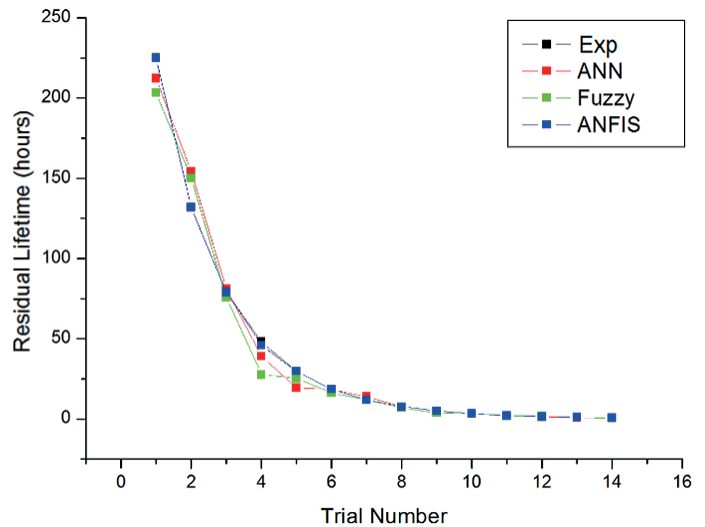


Fig. 13. Comparative analysis of all techniques

8. Conclusion

A humidity sensor based on zinc oxide and carbon has been fabricated and its characterization has been prepared using various tests. Complex impedance spectroscopy shows that electronic conductivity of the sensor is 6.4×10^{-3} S/cm, at the 20% of ZnO and 80% of carbon ratio. Scanning electron microscopy has confirmed the morphology of the composite. XRD and FTIR have confirmed its nature. The humidity

sensor thus fabricated shows good performance and the humidity-sensing range of 30% RH to 95% RH. The residual lifetime of the sensor is calculated using the accelerated life testing technology and an expert system is modelled using a variety of artificial intelligence methods. Amongst all the intelligent modelling techniques, ANFIS proves the most accurate one, with an error rate of 1.1%, whereas for ANN the rate stands at 9.33% and for FIS it is 14.07%.

REFERENCES

- [1] W.J. Roesch, "Historical review of compound semiconductor reliability," *Microelectronics Reliability*, 46(8), 1218–1227 (2006).
- [2] M. Nazari, S. Kashanian, P. Moradipour, and N. Maleki, "A novel fabrication of sensor using ZnO-Al₂O₃ ceramic nanofibers to simultaneously detect catechol and hydroquinone," *Journal of Electroanalytical Chemistry*, 812(122–131) (2018).
- [3] A.E.H. Isaaq, H.M. Elkhair, A.A. Elbadawi, M.A. Siddig, and M.K.S. Elkhair, "Determination of Dielectric Constant of Gum Arabic/Carbon Black Composite Material," *Nova Journal of Engineering and Applied Sciences*, 4(1), (2016).
- [4] B.R. Sankapal, H.B. Gajare, S.S. Karade, R.R. Salunkhe, and D.P. Dubal, "Zinc oxide encapsulated carbon nanotube thin films for energy storage applications," *Electrochimica Acta*, 192, 377–384 (2016).
- [5] S.S. Kumar, P. Venkateswarlu, V.R. Rao, and G.N. Rao, "Synthesis, characterization and optical properties of zinc oxide nanoparticles," *International Nano Letters*, 3(1), 30 (2013).
- [6] M. Kumar and C. Sasikumar, "Electrodeposition of Nanostructured ZnO Thin Film: A," *American Journal of Materials Science and Engineering*, 2(2), 18–23 (2014).
- [7] H. Khawal, U. Gawai, K. Asokan, and B. Dole, "Modified structural, surface morphological and optical studies of Li 3+ swift heavy ion irradiation on zinc oxide nanoparticles," *RSC Advances*, 6(54), 49068–49075 (2016).
- [8] S. Shanthi, S. Poovaragan, M. Arularasu, S. Nithya, R. Sundaram, C.M. Magdalane, K. Kaviyarasu, and M. Maaza, "Optical, Magnetic and Photocatalytic Activity Studies of Li, Mg and Sr Doped and Undoped Zinc Oxide Nanoparticles," *Journal of nanoscience and nanotechnology*, 18(8), 5441–5447 (2018).
- [9] K.I.M. Sinteza, N. Uporabe, T.K.E. Galun-Lete, and I. Pepel, "Synthesis, Characterization and Sensing Application of a Solid Alum/Fly Ash Composite Electrolyte," *Materiali in tehnologije*, 47(4), 467–471 (2013).
- [10] T. Fei, K. Jiang, S. Liu, and T. Zhang, "Humidity sensors based on Li-loaded nanoporous polymers," *Sensors and Actuators B: Chemical*, 190(523–528) (2014).
- [11] P.-G. Su and W.-Y. Tsai, "Humidity sensing and electrical properties of a composite material of nano-sized SiO₂ and poly (2-acrylamido-2-methylpropane sulfonate)," *Sensors and Actuators B: Chemical*, 100(3), 417–422 (2004).
- [12] S. Jose, F. Voogt, C. van der Schaar, S. Nath, N. Nenadović, F. Vanheltmont, E.J. Lous, H. Suy, M. in't Zandt, and A. Šakić, "Reliability tests for modelling of relative humidity sensor drifts". Reliability Physics Symposium (IRPS), *2017 IEEE International: IEEE*; 2017:4A-4.1–4A-4.4.
- [13] K.A. Kaiser and N.Z. Gebraeel, "Predictive maintenance management using sensor-based degradation models," *IEEE Transactions on Systems, Man, and Cybernetics-Part A: Systems and Humans*, 39(4), 840–849 (2009).
- [14] J. Aggarwal and C. Bhargava, "Reliability Prediction of Soil Humidity Sensor using Parts Count Analysis Method," *Indian Journal of Science and Technology*, 9(47), (2016).
- [15] S. Zhao, V. Makis, S. Chen, and Y. Li, "Evaluation of Reliability Function and Mean Residual Life for Degrading Systems Subject to Condition Monitoring and Random Failure," *IEEE Transactions on Reliability*, 67(1), 13–25 (2018).
- [16] A. Ghasemi, S. Yacout, and M.-S. Ouali, "Evaluating the reliability function and the mean residual life for equipment with unobservable states," *IEEE Transactions on Reliability*, 59(1), 45–54 (2010).
- [17] Z. Tian, "An artificial neural network method for remaining useful life prediction of equipment subject to condition monitoring," *Journal of Intelligent Manufacturing*, 23(2), 227–237 (2012).
- [18] N. Fard and C. Li, "Optimal simple step stress accelerated life test design for reliability prediction," *Journal of statistical planning and inference*, 139(5), 1799–1808 (2009).
- [19] X. Huang, P.M. Denprasert, L. Zhou, A.N. Vest, S. Kohan, and G.E. Loeb, "Accelerated life-test methods and results for implantable electronic devices with adhesive encapsulation," *Bio-medical Microdevices*, 19(3), 46 (2017).
- [20] V. Naikan and A. Rathore, "Accelerated temperature and voltage life tests on aluminium electrolytic capacitors: A DOE approach," *International Journal of Quality & Reliability Management*, 33(1), 120–139 (2016).
- [21] C. Bhargava, V.K. Banga, and Y. Singh, "Failure prediction and health prognostics of electronic components: A review". *Engineering and Computational Sciences (RAECS)*, 2014 Recent Advances in: IEEE; 2014:1–5.
- [22] C. Bhargava, V.K. Banga, and Y. Singh, "Reliability Comparison of a Fabricated Humidity Sensor using Various Artificial Intelligence Techniques," *International Journal of Performability Engineering*, 13(5), 577 (2017).
- [23] S.M. Virk, A. Muhammad, and A. Martinez-Enriquez, "Fault prediction using artificial neural network and fuzzy logic", Artificial Intelligence, 2008. MICAI'08. Seventh Mexican International Conference on: IEEE; 2008:149–154.
- [24] M. Lefik, "Some aspects of application of artificial neural network for numerical modeling in civil engineering," *Bulletin of the Polish Academy of Sciences: Technical Sciences*. 61(1), 39–50 (2013).
- [25] D. Rajeev, D. Dinakaran and S. Singh, "Artificial neural network based tool wear estimation on dry hard turning processes of AISI4140 steel using coated carbide tool," *Bull. Pol. Ac.: Tech.*, 65(4), 553–559 (2017).
- [26] C.S. Byington, M. Watson, and D. Edwards, "Data-driven neural network methodology to remaining life predictions for aircraft actuator components", Aerospace Conference, 2004. Proceedings, 2004 IEEE, Vol 6: IEEE; 2004:3581–3589.
- [27] Z. Tian, L. Wong, and N. Safaei, "A neural network approach for remaining useful life prediction utilizing both failure and suspension histories," *Mechanical Systems and Signal Processing*, 24(5), 1542–1555 (2010).
- [28] I. Mansouri, A. Gholampour, O. Kisi, and T. Ozbakkaloglu, "Evaluation of peak and residual conditions of actively confined concrete using neuro-fuzzy and neural computing techniques," *Neural Computing and Applications*, 29(3), 873–888 (2018).
- [29] M. Simulink and M. Natick, "The mathworks": Inc; 1993.
- [30] M. Golob and B. Tovornik, "Input–output modelling with decomposed neuro-fuzzy ARX model," *Neurocomputing*, 71(4), 875–884 (2008).

- [31] E.D. Kirby and J.C. Chen, "Development of a fuzzy-nets-based surface roughness prediction system in turning operations," *Computers & Industrial Engineering*, 53(1), 30–42 (2007).
- [32] C. Chen, B. Zhang, and G. Vachtsevanos, "Prediction of machine health condition using neuro-fuzzy and Bayesian algorithms," *IEEE Transactions on instrumentation and Measurement*, 61(2), 297–306 (2012).
- [33] K. Sathiyasekar, K. Thyagarajah, and A. Krishnan, "Neuro fuzzy based predict the insulation quality of high voltage rotating machine," *Expert Systems with Applications*, 38(1), 1066–1072 (2011).
- [34] D. Nauck and R. Kruse, "A neuro-fuzzy method to learn fuzzy classification rules from data," *Fuzzy sets and Systems*, 89(3), 277–288 (1997).
- [35] G. Manogaran, R. Varatharajan and M. Priyan, "Hybrid recommendation system for heart disease diagnosis based on multiple kernel learning with adaptive neuro-fuzzy inference system," *Multimedia tools and applications*, 77(4), 4379–4399 (2018).
- [36] O. Dragomir, R. Gouriveau, and N. Zerhouni, "Adaptive Neuro-Fuzzy inference system for mid term prognostic error stabilization", International Conference on Computers, Communications & Control, ICCCC'08, Vol 32008:271–276.